Thin Solid Films 534 (2013) 348–355

Contents lists available at SciVerse ScienceDirect

Thin Solid Films

journal homepage: www.elsevier.com/locate/tsf

Detailed analysis of defect reduction in electrowetting dielectrics through a two-layer 'barrier' approach

A. Schultz [a], S. Chevalliot [a,b], S. Kuiper [c], J. Heikenfeld [a,*]

[a] School of Electronic and Computing Systems, Novel Devices Laboratory, The University of Cincinnati, Cincinnati, OH, 45221, USA
[b] Varioptic, 24B rue Jean Baldassini, 69007 Lyon - France
[c] Optilux Inc., 1735 East Bayshore Road, Unit 8B Redwood City, CA 94063, USA

ARTICLE INFO

Article history:
Received 27 August 2012
Received in revised form 27 February 2013
Accepted 1 March 2013
Available online 20 March 2013

Keywords:
Electrowetting
Dielectric
Interfacial tension
Parylene

ABSTRACT

Low-voltage electrowetting requires a thin dielectric capacitor and field strengths approaching 1 MV/cm. Unlike traditional metal/dielectric/metal capacitors, the conducting electrowetted liquid can electrically propagate through the smallest dielectric defects or pores, even for the best barrier polymers such as Parylenes, leading to catastrophic failure such as electrolysis. A detailed analysis of double layer dielectric systems is shown to provide >100 times reduction in defect density, with >10 cm^2 area exhibiting no dielectric failure at >2 times the required electrowetting voltage. An anodized-Al_2O_3/Parylene-HT stack provides electrowetting contact angle modulation down to saturation at 70° at <15 V with breakdown protection to >3 times that voltage. These results build on previous findings on the effect of ion type, liquid type, polymer dielectric choice, electrode material, and provide a next major advance in electrowetting reliability.

© 2013 Elsevier B.V. All rights reserved.

1. Introduction

Electrowetting [1] is well known for its use in applications ranging from optics [2–4], to displays [5,6], to lab-on-chip [7–9]. Reliable electrowetting is commercially proven, a prime example being the Varioptic Artic 316 'liquid lens' product which provides $>10^8$ switching cycles with a several μm-thick Parylene dielectric and 60 V_{RMS} operation. Low-voltage (<15 V) operation has also been demonstrated by several research groups using higher capacitance dielectrics, as recently reviewed by Liu et al. [10]. However, largely unpublished are the very short operating lifetimes (minutes) and low fabrication yields (>1 catastrophic defect/cm^2) for such attempts. Device degradation often takes on the form of electrolysis (Fig. 1a) or electrochemical attack of the underlying electrode.

There are several factors that cause low-voltage electrowetting to be particularly challenging. First, as you decrease the dielectric thickness, the required voltage decreases as only the square root of thickness, causing the required electric field to *increase* [11]. For example, modulation of contact angle from 180° to 70° with 15 V in an oil/water system of 15 mN/m interfacial tension, requires a Parylene dielectric that is ~150 nm thick, and therefore highly stressed under an electric field of ~1 MV/cm. Further problematic, unlike traditional metal/dielectric/metal capacitors, the conducting electrowetted liquid can electrically propagate through the dielectric, using even the smallest of defects or pores in the dielectric. In addition, most electrowetting devices require dielectric areas of 1's to 100's of cm^2 area, so <1 dielectric defect per cm^2 is realistically a minimum requirement, with <1 per 100–1000 cm^2 preferred.

Motivated by frustration in watching our own low-voltage devices electrically deteriorate, sometimes in a manner of seconds or minutes, we began an in-depth study of all the factors that might be related to improving electrowetting reliability. In 2009, we showed that substitution of large organic ions for small inorganic ones can reduce dielectric failure if dielectric defects/pores are too small to transport large ions [12]. In 2010, we published results on Parylene HT (fluorinated), which compared to conventional Parylenes showed improved dielectric reliability at 300 nm thickness, and extreme resistance to charge injection under a DC voltage stress of several hours [13]. In 2011, our studies expanded to large molecule and less electrochemically reactive non-aqueous electrowetting liquids, made properly conductive with large organic salts [14]. Also, in 2011, we introduced the concept of a self-healing (regenerating) dielectric by using an underlying Al electrode and acidic anodizing electrowetting liquid, to generate Al_2O_3 at dielectric defects [15] which was similarly demonstrated by using only a very thin (20–110 nm) fluoropolymer layer with anodic voltages [16]. However, this concept is limited to applications that can be operated with DC voltage or AC voltage with DC offset. That same year, we demonstrated that if good materials and typical voltage conditions are used, electrowetting saturation is not due to effects such as dielectric charging, and is invariant to materials parameters [17]. Despite these efforts, our large-area and low-voltage electrowetting devices, especially those used for displays, still exhibited too many dielectric failures to be considered useful from an applied perspective. Degradation occurred even when using the best available dielectrics such as those deposited by atomic layer deposition.

* Corresponding author. Tel.: +1 513 556 4763; fax: +1 513 556 7326.
E-mail address: heikenjc@ucmail.uc.edu (J. Heikenfeld).

0040-6090/$ – see front matter © 2013 Elsevier B.V. All rights reserved.
http://dx.doi.org/10.1016/j.tsf.2013.03.008

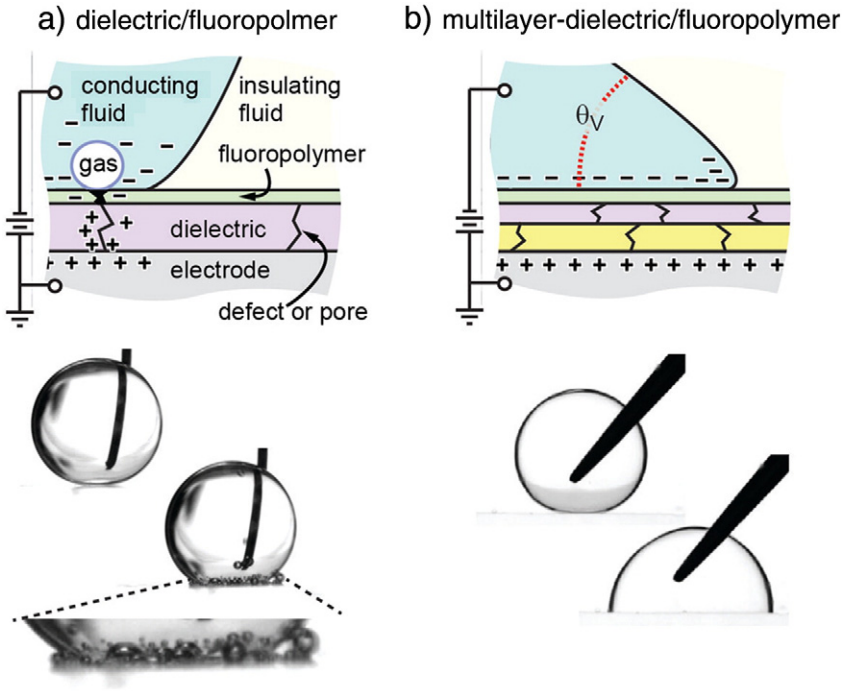


Fig. 1. Diagrams and photos of (a) a failed single-layer electrowetting dielectric exhibiting electrolysis; (b) improved operation with a multi-layer dielectric that does not exhibit dielectric failure.

An additional materials advance is clearly needed to reduce the density of defects in electrowetting dielectrics, ideally using a fabrication approach that is both highly economical and deposited at or near room-temperature. We report here a detailed analysis of significant defect reduction in electrowetting dielectrics through a simple double-layer 'Barrier' approach. We observe >100 times reduction in defect density compared to single layer dielectrics, with >10 cm^2 area exhibiting no dielectric failure at >2 times the operating voltage. A simple anodized Al_2O_3/Parylene-HT stack provides electrowetting contact angle modulation down to 70° at <15 V with no dielectric failure at up to >3 times that voltage. Although not the only investigation of multi-layer electrowetting dielectrics [18,19], this expands on previous investigations to address important issues such as defect density, and to examine the materials requirements in detail. Furthermore, our experimental evidence suggests that the improved dielectric performance may not be due to the organic dielectric filling or passivation of defects in the underlying dielectric, as suggested by Lin et al. [18]. Rather, it appears that the improvement is due to creating a tortuous path for liquid/ion penetration (Fig. 1b), which is analogous to multi-layer inorganic/organic gas/moisture barriers developed for encapsulation of organic light emitting diode displays [20,21]. Our results provide a significant advance and build on a large cumulative body of work toward reliable low-voltage electrowetting.

2. Experimental methods

Electrowetting tests were performed using simple sessile droplet tests similar to that shown in Fig. 1. Sodium dodecyl sulfate (SDS) was added to de-ionized water to create the conducting test liquid. SDS is well characterized in electrowetting systems and provides a mechanism to test the effect of ion-size on dielectric failure [12,13]. With positive voltage to the aqueous solution, the small sodium cations ($Na+$) will be responsible for dielectric failure, whereas with negative voltage, it is the large dodecyl sulfate anions. Although non-aqueous solutions are preferred for improved reliability in displays or optics [14], aqueous solution was tested because it is often required for some electrowetting applications such as lab-on-chip (chemical properties) and liquid lenses (optical properties). The oil tested was OS-30 silicone oil from Dow Corning.

Two types of dielectric failure tests were performed. Small area (~0.5 cm^2) tests were designed for investigating resistance to failure due to the more homogeneous nature of the dielectric film (i.e. none or few of the large-size defects). These tests were carried out in air using a 0.7 μm Platinum probe and 1 μL, 0.01 wt.% SDS solution droplets. These experiments are always performed in air (not insulating oil) because that makes the droplet less mobile due to contact angle hysteresis. Without contact angle hysteresis, at higher voltages, inhomogeneous charging of the dielectric can cause the droplet to spontaneously leap away from the probe. DC voltage was applied at a slow step rate of ±1 V/s up to ±98 V with the electrode under the dielectric grounded. This slow step rate is needed for electrowetting reliability testing because dielectric failure mechanisms typically evolve over time (e.g. are not due to classical electrical breakdown). Five droplets per dielectric sample were tested and the current was recorded every 1 volt. Dielectric failure was attributed to current exceeding a value of ±1 μA.

A second, large area test, was implemented to capture dielectric failure due to large and inhomogeneous dielectric features (defects). The same SDS solution was confined over an area of ~100 cm^2 with use of a polydimethysiloxane gasket and a glass plate with a transparent In_2O_3:SnO_2 bias electrode. The transparent top plate allowed photographic capture of breakdown, observed by bubble formation (electrolysis). For the large area tests, a very slow ramp rate of 1 V/5 s was applied up to 30 V with the maximum current clamped to <10 mA. Top-view photos were taken every 1 V and combined sequentially into a video [22]. Simultaneously, electrical current was measured to further quantify the magnitude of dielectric failure.

A large variety of single-layer and two-layer dielectrics were tested in order to reveal what characteristics promote a reliable multi-layer dielectric (Table 1). For all experiments, borosilicate glass substrates were first sputter-deposited with a ~400 nm Al electrode. Thicker Al was utilized in some experiments, so that an Al_2O_3 dielectric could be formed by room-temperature anodization in an electrolytic ammonium phosphate solution (~2 wt.%, ~2 nm/V). Organic dielectrics were also tested, including Parylene C (chlorinated) and Parylene HT (fluorinated). Both

Table 1
Tested single-layer and multi-layer dielectrics. The Cytop fluoropolymer has little influence on electrowetting reliability (explained elsewhere in this paper) and is not counted in the 'single' or 'double' nomenclature.

Single layer
150 nm Al_2O_3/50 nm Cytop
300 nm SU-8/50 nm Cytop
50 nm Parylene C/50 nm Cytop
50 nm Parylene HT/50 nm Cytop
Two layer
150 nm Al_2O_3/50 nm Parylene C/50 nm Cytop
150 nm Al_2O_3/50 nm Parylene HT/50 nm Cytop
300 nm SU-8/50 nm Parylene C/50 nm Cytop
300 nm SU-8/50 nm Parylene HT/50 nm Cytop
50 nm Parylene C/50 nm Parylene HT/50 nm Cytop

Parylene types were respectively deposited at room-temperature by chemical vapor deposition in a Specialty Coating Systems PDS2010 or PDS2035CR lab coater. MicroChem's SU-8 2000 series negative epoxy photoresist was also tested as a dielectric because it has been reported to have very high breakdown field [23], possibly because it is re-melted after spin-coating and solvent evaporation, and then cross-linked with UV exposure. The SU-8 and Parylenes were all processed using their standard manufacturer-stated conditions. In addition, all single-layer and multi-layer dielectric samples were spin coated with 50 nm Asahi Glass Cytop fluoropolymer using 1 wt.% Cytop 809 M and baking at 180 °C for 30 min. This top fluoropolymer layer provides hydrophobicity for a large Young's contact angle, but is not required if an insulating liquid (oil) has an interfacial tension that properly matches the top dielectric surface [13,24].

Before discussing the experimental results, there are two brief but important topics to be discussed. First, the top fluoropolymer layer is not counted toward preventing dielectric failure in any of the experiments. If placed on a second high-quality dielectric, the porosity of thin fluoropolymers is adequately low to allow electrowetting. However, when deposited at thicknesses (<100–200 nm) required for low-voltage operation, we have observed that the porosity/defectivity for all solution-deposited fluoropolymers (Cytop 809 M, Teflon AF 1600, Fluoropel 1601 V, etc.) is too high to provide any meaningful improvement in the reliability of a stack of dielectrics. Furthermore, with the correct choice of dielectric and insulating oil, no fluoropolymer is needed [24]. A second topic relates to the choice of using anodically grown Al_2O_3, which is inherently electrochemically porous by nature of the anodization. It therefore is an ideal dielectric to investigate if multi-layer dielectrics would provide any improvement to reliability. We disagree with the conclusions of Lin et al., [18] who stated: "Among the materials tested, the dielectric constants of Al_2O_3 and Si_3N_4 are too low for practical use." We will show that the comparatively low dielectric constants of Al_2O_3 and Si_3N_4 are suitable enough for low-voltage electrowetting with a stacked electrowetting dielectric. Furthermore, higher dielectric constant materials are often less electrochemically stable, need to be thicker (more strain, defects), exhibit stronger charge trapping/hysteresis.

Lastly, we note that beyond Al electrode coating, all additional fabrication processes were performed under the most challenging case: a non-cleanroom environment without climate control. Both the anodization and Parylene coating techniques are resilient to particulates and surface contamination, such that any reliable films achieved should be easily reproduced by others.

3. Theoretical expectations

No dielectric stack is useful if the electrical field across any individual layer in the stack exceeds its bulk electrical breakdown limit. Using an insulator with a high dielectric constant in combination with a dielectric with a low dielectric constant leads to field amplification in the layer with the low constant. In practical situations, this often leads to breakdown of the latter. This was pointed out by Kuiper et al. [11] Previous theoretical plots do not account for electrical breakdown limits, nor do they account for how a defect in one layer can cause the entire voltage drop to appear across the other layer [24,25]. The following derivations provide suitable ranges within which the experiments were performed.

The required voltage (V) can be derived from the electrowetting equation [26]: $cos\theta_V = (\gamma_{id} - \gamma_{cd})/\gamma_{ci} + (C{\cdot}V^2)/(2{\cdot}\gamma_{ci})$, (1), where C is the dielectric capacitance and the γ terms are the interfacial tensions between the conducting (c), insulating (i) liquid, and the dielectric (d). Using simple series capacitor equations, two limiting cases can be derived: no defects, $E_{layer} = (V{\cdot}C_{tot})/(C_{layer}{\cdot}d_{layer})$, (2), and a defect in layer 1, $E_{layer2} = V/d_{layer2}$, (3), where each term with subscript 'layer' is the electric field (E), capacitance (C), or thickness (d) for that respective layer.

A challenging and practically relevant case will be chosen: γ_{ci} =30 mN/m and electrowetting from $(\gamma_{id} - \gamma_{cd})/\gamma_{ci} = -1$ ($\theta = 180º$) to $\theta_V = 70º$. Fig. 2a plots the theoretical electric field across a 150 nm Al_2O_3 layer and a Parylene HT layer as the Parylene HT thickness is varied (Eq. 2, blue and red lines). The electric field across the Al_2O_3 layer is also plotted for the case of a defect in the Parylene HT layer (Eq. 3, black line). Fig. 2b is similar, but Parylene HT is fixed at 100 nm and instead, the Al_2O_3 thickness is varied. 2 MV/cm is assumed as the breakdown field for both dielectrics with a liquid electrode, indicated by the horizontal green line. Blue dotted lines represent a limiting window to avoid dielectric failure. Several key conclusions are as follows. Firstly, if the Parylene HT layer is made too thick and has a defect in it, the Al_2O_3 layer will experience the entire applied voltage at that defect.

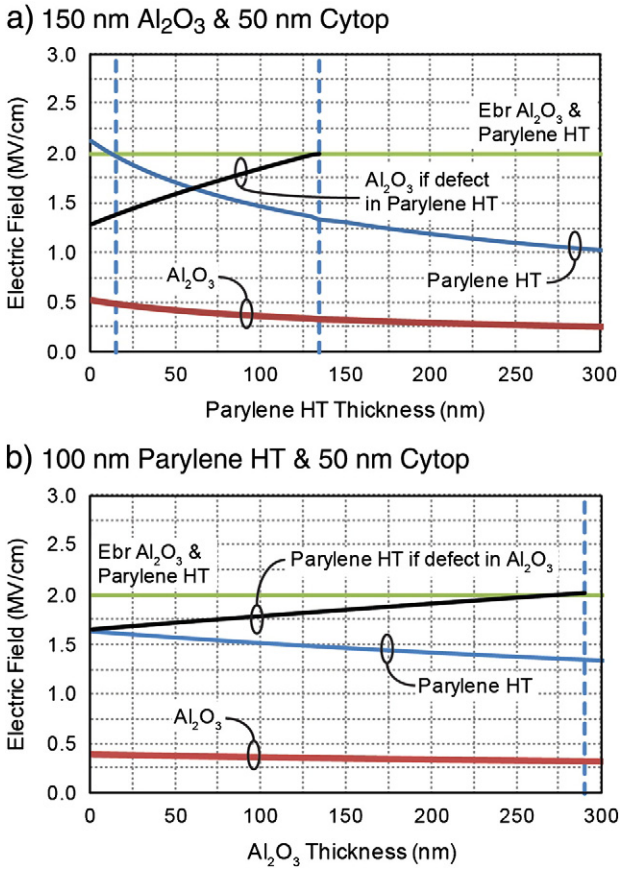


Fig. 2. Plots of theoretical electric fields across the different dielectric layers vs. (a) Parylene HT thickness with 150 nm Al_2O_3 and 50 nm Cytop with, and vs. (b) Al_2O_3 thickness with 100 nm Parylene HT and 50 nm Cytop.

This would likely cause the Al_2O_3 layer to exceed its breakdown field and thereby causing complete dielectric failure (Fig. 2a). Secondly, Al_2O_3 thickness is a less important factor. Thirdly, if the data were replotted for $\gamma_{ci} = 50$ mN/m (not shown), as is the case for some lab-on-chip applications, there would be no reliable operating window! These theoretical plots show that careful consideration of dielectric thickness must be made if thin dielectrics are used to achieve low-voltage operation. For further investigation, an Excel spreadsheet is provided which calculates the electric fields across various layers, with and without the presence of defects in any particular layer [22].

4. Experimental results

Theoretical investigations aided the selection of materials and thicknesses listed in Table 1. The SU-8 was implemented thicker than Parylene despite the high breakdown field of SU-8, because it is generally difficult to make impermeable dielectrics by spin or dip coating.

Fig. 3 plots small area droplet tests on the single-layer dielectrics listed in Table 1. The polarity dependence of dielectric failure is consistent with our previous conclusions on self-healing by anodization [15], and ion size (large dodecyl sulfate anion vs. small Na + [12]), with more subtle effects possible due to Debye screening within pores or defects. The most challenging test is positive bias (Na+), where all dielectrics performed very poorly individually. Even if the dielectrics performed well in negative bias due to anodization of the underlying aluminum electrode, the results cannot be applied to all electrowetting applications since DC (mono-polar) operation of electrowetting devices can lead to long-term charging and ion migration. These results also confirm our initial assumption that the Cytop layer does not significantly contribute to preventing breakdown with a liquid electrode (with a solid electrode it should sustain ~10 V). With a clear indication that these single-layer dielectrics were insufficient for reliable operation, the experiments next turned to two-layer inorganic/organic dielectrics.

Figs. 4 and 5 plot small area droplet tests on Al_2O_3/Parylene and SU-8/Parylene dielectric stacks, respectively. Only Parylene HT exhibited the desired level of reliability. Although much thinner in this work, our previous results have similarly shown that at 300 nm Parylene HT is more reliable than Parylene C [13]. It must, however, be noted that Parylene C was heated to 180 °C for 30 min, whereas the short-term (24 h) service temperature is only 100 °C. It is not clear how this has affected the performance of Parylene C. The short-term service temperature for Parylene HT is 450 °C, which makes it likely that its performance was not influenced by the 180 °C treatment. For the Al_2O_3/Parylene HT (Fig. 4) and SU-8/Parylene HT (Fig. 5) results, the dielectric failure occurs at ~65–70 V on average, which is ~2 times and ~4 times, respectively, the sum of the voltages for failure for each dielectric individually (Fig. 3). It is clear that combining these dielectrics provides an enhancement in reliability that none of these dielectrics has individually.

The small ~0.5 cm^2 area droplet tests of Figs. 3 and 4 clearly show value of stacked dielectrics, particularly with Parylene HT top-layers. These samples show resistance to failure due to the more homogeneous nature of the dielectric stack. Next, 200 times larger area was tested to assess dielectric failure due to larger and inhomogeneous dielectric defects.

Fig. 6 shows brightness and contrast adjusted photographs of dielectric failure for large-area samples (3.8×2.6 cm^2). Ambient white light was enough illumination to allow light scattering from gas bubbles formed at major dielectric defects (electrolysis). It should be noted that a defect generating the 1 μA of current for the plots in Figs. 3–5 does not necessarily lead to gas bubble sizes large enough to visualize in

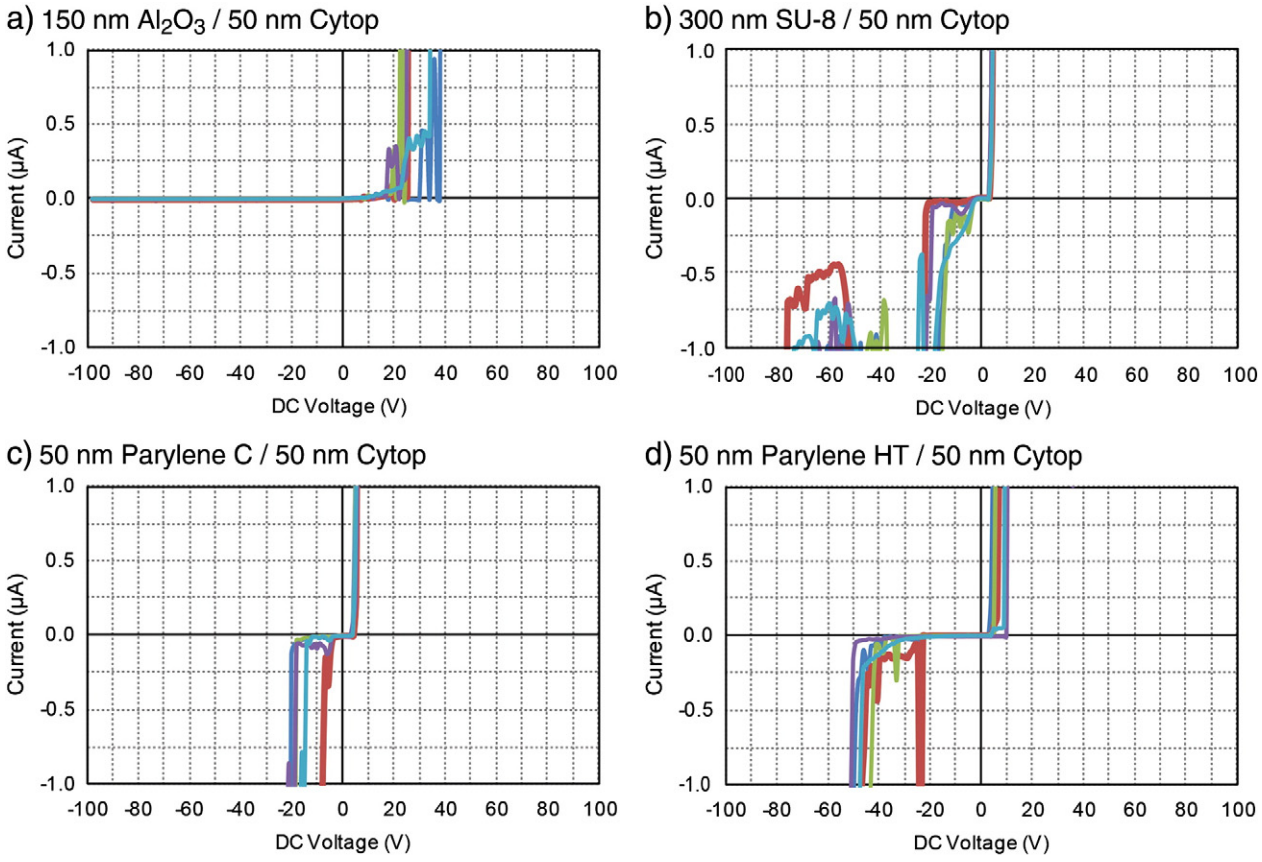


Fig. 3. Plots of current vs. voltage (1 V/s ramp) for (a) 150 nm Al_2O_3/50 nm Cytop, (b) 300 nm SU-8/50 nm Cytop, (c) 50 nm Parylene C/50 nm Cytop, and (d) 50 nm Parylene HT/50 nm Cytop. The Al electrode was grounded and the test solution was 0.01 wt.% SDS in water surrounded by air.

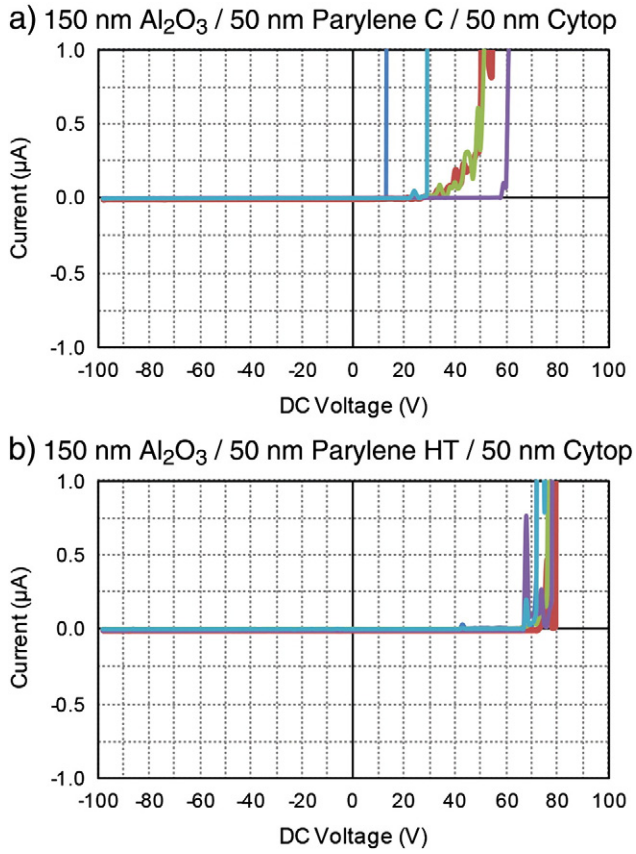


Fig. 4. Plots of current vs. voltage (1 V/s ramp) for (a) 150 nm Al_2O_3/50 nm Parylene C/50 nm Cytop, and (b) 150 nm Al_2O_3/50 nm Parylene HT/50 nm Cytop. The Al electrode was grounded and the test solution was 0.01 wt.% SDS in water surrounded by air.

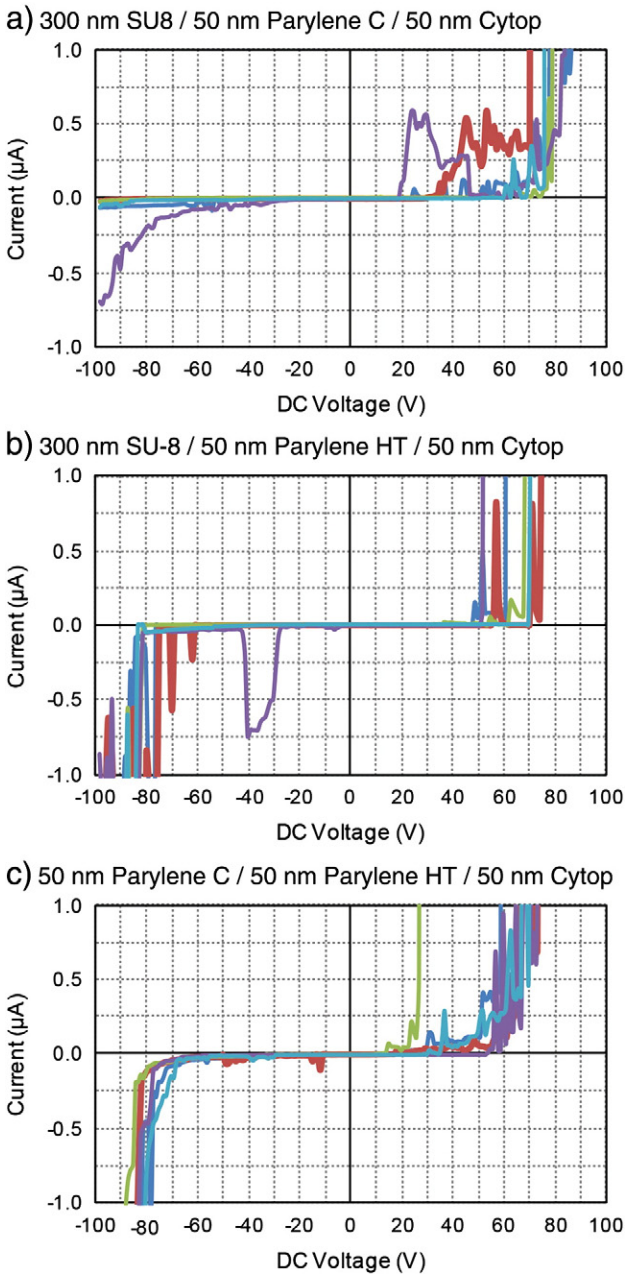


Fig. 5. Plots of current vs. voltage (1 V/s ramp) for (a) 300 nm SU-8/50 nm Parylene C/50 nm Cytop, and (b) 300 nm SU-8/50 nm Parylene HT/50 nm Cytop. The Al electrode was grounded and the test solution was 0.01 wt.% SDS in water surrounded by air.

the photographs of Fig. 6. Therefore, the results of Fig. 6 should be analyzed independently of the previous discussion and conclusions.

It is visually obvious that all of the single-layer dielectrics (Fig. 6a–c) exhibit an intolerable density of major defects even at 10 V, which corresponds to electric fields below bulk breakdown fields in each layer for every sample tested. An ideal goal would be that no defects should cause dielectric failure for at least 2 times the targeted operation voltage of <15 V. Fig. 6d-e are for the Al_2O_3/Parylene stacks which exhibited very few major defects, if any at all for Al_2O_3/Parylene HT. For the Al_2O_3/Parylene HT test, few points of light scattering existed at 0 V and did not change with voltage, and therefore are just due to particulates (e.g. no dielectric failure). The number of gas bubbles present for each 1 V step was counted using Image J software from every sample shown in Fig. 6, and the data are plotted in Fig. 7. It should be noted that the defect count above ~15 V for the single-layer cases were difficult to discern due to coalescence of larger bubbles and spreading of small bubbles over the entire surface where there were no visible defects. The complete absence of bubble generation for Al_2O_3/Parylene HT, over a large area of ~100 cm^2, for the challenging case of positive voltage (small Na+) at 30 V and 150 s, and even up to 40 V and 200 s (not shown), is unlike any result we have previously observed or seen reported for such a thin dielectric stack. Even the Al_2O_3/Parylene C results are highly encouraging, and may prove valuable to those who do not have access to Parylene HT coating capability.

It is obvious that the tested single-layer dielectrics do not electrically compare to those of the stacked dielectrics when considering the capacitances. Therefore, for completeness of understanding, single-layer Parylene HT large area samples with thicknesses chosen to match the capacitance of the stacked Al_2O_3/Parylene HT sample were also tested. With Parylene HT thickness of 87 nm, the results were only slightly better than the single-layer Parylene HT sample already mentioned. This further demonstrated value in using multi-layer dielectrics for reducing voltage and improving reliability.

Fig. 8 shows the results of a film stack developed specifically for <15 V operation. The Al_2O_3 layer was reduced in thickness to 100 nm, simply for convenience (e.g. less Al required, shorter process time, reduced potential strain in the film). Small droplet area current–voltage plots were again taken and confirmed that 100 nm Al_2O_3 seems to perform as well as 150 nm (Fig. 8a). In Fig. 8b, the SDS surfactant was increased from the 0.01 wt.% used in other experiments to 100 times higher (1.0 wt.%). This lowers the interfacial tension to ~8.5 mN/m and therefore allows lower operating voltage. However, this also shows a much more challenging test as we have always observed that higher ion concentration reduces dielectric reliability. Even at this much higher wt. %, the system did not exhibit dielectric failure until 40–50 V. Fig. 8c plots an average of 5 electrowetting curves taken

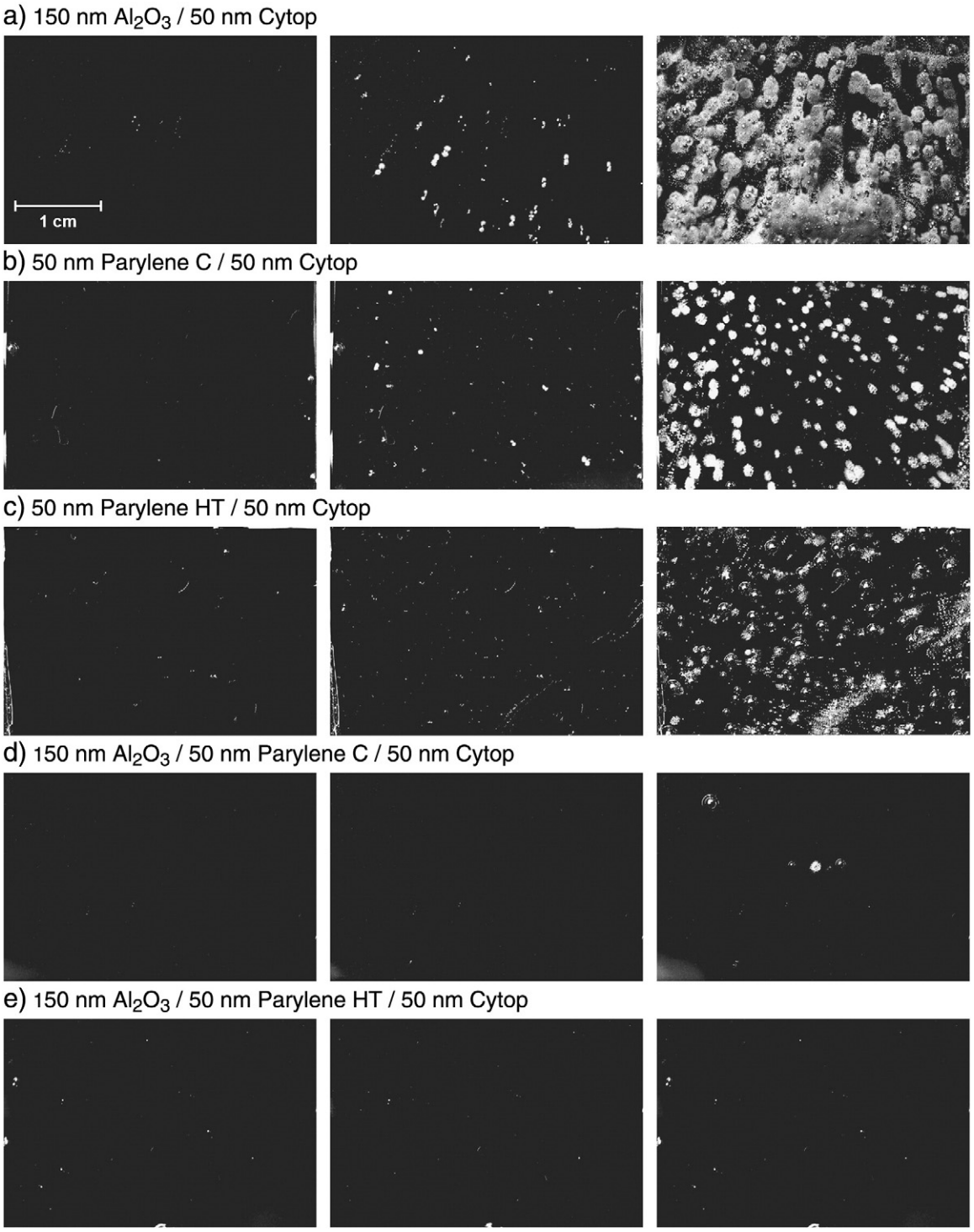


Fig. 6. Adjusted photos of dielectric failure for large area samples at 0 V(t = 0 s), 15 V(t = 50 s) and 30 V(t = 150 s) for (a) 150 nm Al_2O_3/50 nm Cytop, (b) 50 nm Parylene C/50 nm Cytop, (c) 50 nm Parylene HT/50 nm Cytop, (d) 150 nm Al_2O_3/50 nm Parylene C/50 nm Cytop, and (e) 150 nm Al_2O_3/50 nm Parylene HT/50 nm Cytop. The Al electrode was grounded, and the test solution was 0.01 wt.% SDS in water.

with a 120 Hz square wave. Electrowetting down to saturation at 70° is achieved with 14 V, and with no dielectric failure at up to >3 times that voltage.

5. Discussion

The first item of discussion relates to using our previously published advances in reliability [12–14] to improve the results reported herein. Several improvements could push the dielectric failure window to much higher voltages while allowing <15 V electrowetting: (1) SDS could be eliminated and an oil-soluble surfactant used to achieve comparable interfacial tension and operating voltage; (2) use only large ions [12] at the minimum concentration that satisfies the RC time-constant of the system [14]; (3) use non-aqueous (larger molecule) conductive liquids with larger molecules [14]. These experiments, coupled with longer term aging of 10,000 h continuous AC voltage would reveal best practices for long-lasting low-voltage electrowetting operation. Future work should also attempt to elucidate the nature of homogeneous

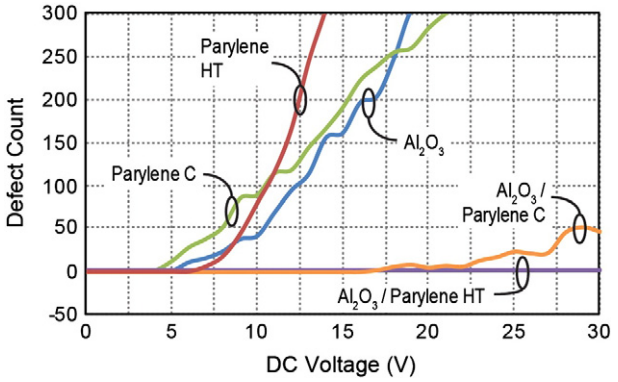


Fig. 7. Count of observed defects vs. voltage (1 V/5 s ramp) for the different large area samples.

and non-homogeneous defects causing dielectric failure in the small vs. large area tests, respectively.

The second item of discussion relates to achieving even lower voltage operation (<1–5 V). Other reports have shown very low-voltage operation using interfacial tensions (<5 mN/m) that are impractical for most applications [25]. Another technique is to use extremely thin dielectric stacks [25,27,28]. We presently doubt that such systems, if forced to use practical interfacial tension values, would exhibit adequate dielectric reliability even with multi-layer enhancement. As described in Fig. 2, the electric field strengths become very high, approaching the conventional breakdown fields of polymers. Based on available literature, we conclude at this point that <15 V operation is therefore state-of-the-art for reliable electrowetting operation with normal surface tension values.

A third item of discussion is to compare the results reported here with the results of Lin et al. [18]. Direct comparisons are not possible, because Lin's paper lacked important information such as duration of voltage application, interfacial tensions, and ion types/concentrations, but some discussion is merited. Firstly, we achieve comparable dielectric reliability, but with a higher capacitance of 17 nF/cm^2 compared to 8 pF/cm^2 for 200 nm Ta_2O_5/200 nm Parylene C/70 nm Cytop [18]. With our previously demonstrated results of using alkane oils and eliminating the need for a Cytop layer [13], the capacitance increases to 32 nF/cm^2 which is ~4 times the previous results and would result in ~7 V electrowetting. However, at such high capacitance liquids and ions would need to be carefully optimized to prevent charge injection into the Parylene HT layer. Lin et al. also speculated that the Parylene, being a highly conformal coating, penetrates defects in the lower dielectric, resulting in the improved dielectric reliability. We designed experiments to explore this possibility by varying the Parylene HT thickness down to just several nm on anodized Al_2O_3. If filling of pores/defects is the cause for improved reliability, it would require only a coating of a few to 10's of nm of Parylene HT. However, thinner Parylene HT simply showed a gradual decrease in reliability over the thickness range of 0–50 nm indicating that this may not be the case. If it was the reason for improved reliability, then no major change in reliability should be observed until the Parylene thickness was less than a few nm thick (in theory, only a few nm should be adequate to fill most pores/defects). More conclusive evidence will be necessary to determine if the plausibility of this speculation holds.

Lastly, we comment on the stacking order or number of stacks. It could be that improved reliability could result from splitting the total thickness of the dielectric into an increased number of thinner alternating layers. If improved performance were achieved, it would likely be due to one of two hypothesis: (1) multi-layer electrowetting dielectrics exhibit a more tortuous pathway for ion migration in the dielectric, similar to multi-layer barrier films for organic electronics [20,29]; (2) the multiple interfaces between inorganic/organic layers create 'traps' for liquid and ions attempting migration through the

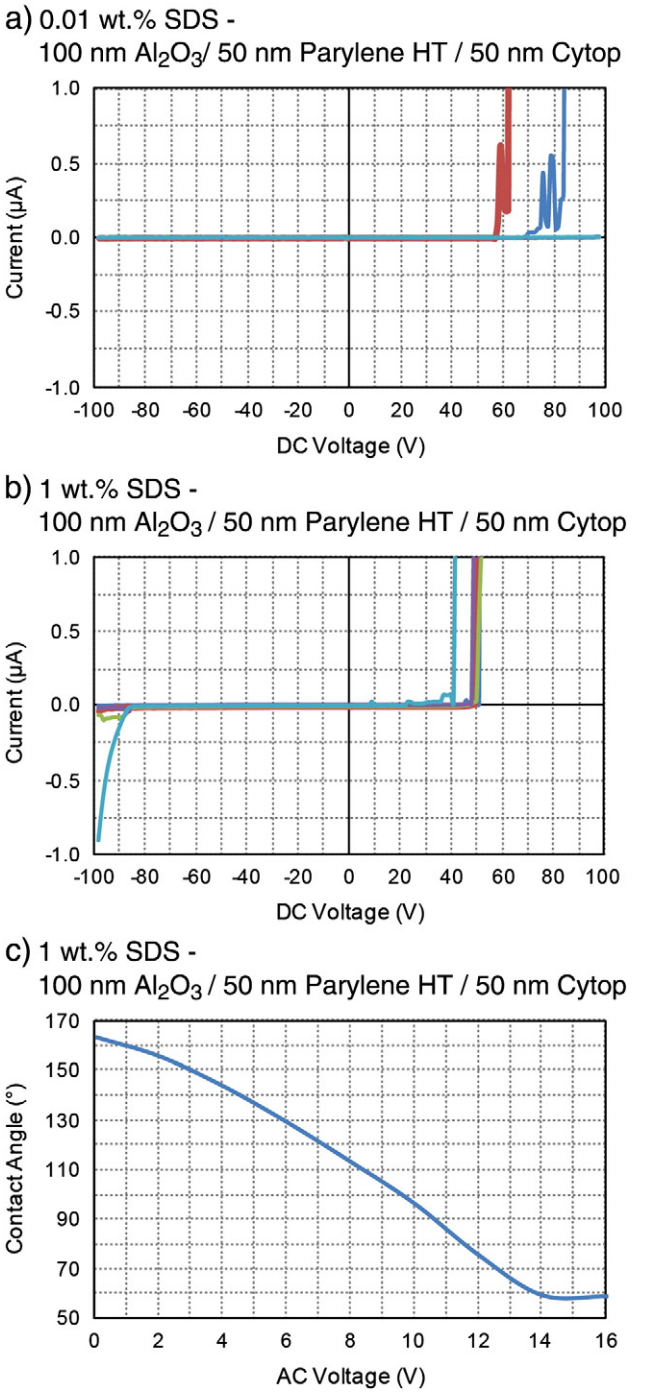


Fig. 8. Plots for 100 nm Al_2O_3/50 nm Parylene HT/50 nm Cytop of current vs. voltage (1 V/s ramp) with (a) 0.01 wt.% SDS and (b) 1 wt.% SDS solutions surrounded by air, and (c) electrowetting contact angle measurements vs. AC voltage with 1 wt.% SDS in silicone oil. The Al electrode was grounded.

dielectric [20]. The latter is less plausible for an electrowetting system, since with only two layers a dramatic increase in performance is observed herein. Such future work may not be necessary, as the initial results shown herein reveal the possibility that the simpler implementation of only two layers might be adequate. Regarding which is the lower dielectric, inorganic or organic, we suggest the inorganic should be the lower dielectric for five reasons: (1) it is the most practical approach if one uses anodization or higher temperature processing to create the inorganic dielectric; (2) if porous type anodized Al_2O_3 is used as the top dielectric, the ions will more easily flow into the pores; (3) less charge trapping is generally expected at the interface

between polymer/fluoropolymer compared to inorganic/polymer; (4) if the fluoropolymer is eliminated, a large Young's angle is more easily achieved if a non-fluorinated but hydrophobic polymer is used as the upper layer; (5) the Papathanasiou group has shown an improvement in the adhesion strength of the hydrophobic top coating to the main dielectric, and improved electrical reliability, when a plasma-deposited fluorocarbon interlayer is provided [19].

6. Conclusions

In conclusion, due to defects or pores in a dielectric layer, electrical breakdown has been a significant but infrequently reported issue in electrowetting systems, especially as the dielectric layer thickness is reduced to achieve low voltage. This work has demonstrated that by employing a multi-layer dielectric, particularly with a Parylene HT upper layer, the dielectric performance is significantly improved for low voltage (<15 V electrowetting systems). The improved performance is far beyond the sum of the performance for the individual dielectric layers, as evidenced for small homogenous dielectric defects (small area tests) and large inhomogeneous dielectric defects (large area tests). The exact mechanism for the improved performance remains unproven, but is speculated to be similar to an increase in tortuosity similar to multi-layer barrier films used for organic electronics.

Acknowledgements

The University of Cincinnati authors gratefully acknowledge partial support from NSF Career award no. 0640964 (University of Cincinnati), NSF IHCS award no. 1001141 as well as help from Specialty Coating Systems, Inc. with Parylene HT and Parylene C.

References

[1] F. Mugele, J.-C. Baret, J. Phys. Condens. Matter 17 (28) (2005) R705.
[2] B. Berge, Micro Electro Mechanical Systems, 2005. MEMS 2005. 18th IEEE International Conference on, 2005, p. 227.
[3] S. Kuiper, in: H. Schenk, W. Piyawattanametha (Eds.), SPIE, San Francisco, California, USA, 2011, p. 793008.
[4] N.R. Smith, D.C. Abeysinghe, J.W. Haus, J. Heikenfeld, Opt. Express 14 (14) (2006) 6557.
[5] J. Heikenfeld, K. Zhou, E. Kreit, B. Raj, S. Yang, B. Sun, A. Milarcik, L. Clapp, R. Schwartz, Nat. Photonics 3 (5) (2009) 292.
[6] R.A. Hayes, B.J. Feenstra, Nature 425 (6956) (2003) 383.
[7] M. Dhindsa, J. Heikenfeld, S. Kwon, J. Park, P.D. Rack, I. Papautsky, Lab Chip 10 (7) (2010) 832.
[8] R. Fair, Microfluid. Nanofluid. 3 (3) (2007) 245.
[9] H. Moon, A.R. Wheeler, R.L. Garrell, J.A. Loo, C.-J. Kim, ldquo, Cj, rdquo Lab Chip 6 (9) (2006) 1213.
[10] H. Liu, S. Dharmatilleke, D. Maurya, A. Tay, Microsyst. Technol. 16 (3) (2010) 449.
[11] S. Kuiper, B. Hendriks, Proceedings of the ESA Annual Meeting 2005, Edmonton, Canada, 2005, p. 28.
[12] B. Raj, M. Dhindsa, N.R. Smith, R. Laughlin, J. Heikenfeld, Langmuir 25 (20) (2009) 12387.
[13] M. Dhindsa, S. Kuiper, J. Heikenfeld, Thin Solid Films 519 (10) (2011) 3346.
[14] S. Chevalliot, J. Heikenfeld, L. Clapp, A. Milarcik, S. Vilner, J. Disp. Technol. 7 (12) (2011) 649.
[15] M. Dhindsa, J. Heikenfeld, W. Weekamp, S. Kuiper, Langmuir 27 (9) (2011) 5665.
[16] M. Khodayari, J. Carballo, N.B. Crane, Mater. Lett. 69 (2012) 96.
[17] S. Chevalliot, S. Kuiper, J. Heikenfeld, J. Adhes. Sci. Technol. 26 (12–17) (2012) 1909.
[18] Y.-Y. Lin, R.D. Evans, E. Welch, B.-N. Hsu, A.C. Madison, R.B. Fair, Sens. Actuators B Chem. 150 (1) (2010) 465.
[19] D.P. Papageorgiou, A. Tserepi, A.G. Boudouvis, A.G. Papathanasiou, J. Colloid Interface Sci. 368 (1) (2012) 592.
[20] L.L. Moro, T.A. Krajewski, N.M. Rutherford, O. Philips, R.J. Visser, M.E. Gross, W.D. Bennett, G.L. Graff, in: Z.H. Kafafi, P.A. Lane (Eds.), SPIE, San Diego, CA, USA, 2004, p. 83.
[21] K. Yamashita, T. Mori, T. Mizutani, J. Phys. D Appl. Phys. 34 (5) (2001) 740.
[22] J. Heikenfeld, p. http://www.ece.uc.edu/devices/NDL_Publications.html.
[23] J. Melai, C. Salm, S. Smits, J. Visschers, J. Schmitz, J. Micromech. Microeng. 19 (6) (2009) 065012.
[24] M. Maillard, J. Legrand, B. Berge, Langmuir 25 (11) (2009) 6162.
[25] S. Berry, J. Kedzierski, B. Abedian, J. Colloid Interface Sci. 303 (2) (2006) 517.
[26] B. Frieder Mugele, Jean-Christophe Baret, J. Phys. Condens. Matter 17 (28) (2005) R705.
[27] H. Moon, S.K. Cho, R.L. Garrell, C.-J.C.J. Kim, J. Appl. Phys. 92 (7) (2002) 4080.
[28] L. Yifan, W. Parkes, L.I. Haworth, A. Ross, J. Stevenson, A.J. Walton, J. Microelectromech. Syst. 17 (6) (2008) 1481.
[29] J. Lewis, Mater. Today 9 (4) (2006) 38.